Editors' Suggestion

Topological Speed Limit

Tan Van Vu* and Keiji Saito†
Department of Physics, Keio University, 3-14-1 Hiyoshi, Kohoku-ku, Yokohama 223-8522, Japan

(Received 22 August 2022; revised 15 November 2022; accepted 5 December 2022; published 4 January 2023)

Any physical system evolves at a finite speed that is constrained not only by the energetic cost but also by the topological structure of the underlying dynamics. In this Letter, by considering such structural information, we derive a unified topological speed limit for the evolution of physical states using an optimal transport approach. We prove that the minimum time required for changing states is lower bounded by the discrete Wasserstein distance, which encodes the topological information of the system, and the time-averaged velocity. The bound obtained is tight and applicable to a wide range of dynamics, from deterministic to stochastic, and classical to quantum systems. In addition, the bound provides insight into the design principles of the optimal process that attains the maximum speed. We demonstrate the application of our results to chemical reaction networks and interacting many-body quantum systems.

DOI: 10.1103/PhysRevLett.130.010402

Introduction.—Investigating how fast a system can evolve is one of the central problems in classical and quantum mechanics. In a seminal work by Mandelstam and Tamm [1], a fundamental bound on the operational time required for the transformation between two orthogonal states for unitary dynamics was derived. Since then, generalizations of the bound for arbitrary states and non-unitary dynamics have been intensively studied [2–36], leading to the notion of speed limits (see Ref. [37] for a review). These speed limits establish the ultimate rate at which a system can evolve to a distinguishable state and have found diverse applications, for example, in quantum control [38–41], quantum metrology [42,43], and thermodynamics of computation [33,44–49].

Interacting systems generally form topological structures in their dynamics, such as chemical reaction networks that consist of several species (see the schematic in Fig. 1). In general, a state represented by a vector $\boldsymbol{x}_t$ evolves over time and is significantly affected by the topology of the dynamics. For instance, a Markov jump process with dense connectivity may relax toward an equilibrium state faster than one with sparse connectivity. A many-body system with long-range interactions can change quantum states faster than one with short-range interactions [50]. Although speed limits for state transformations have been intensively investigated, the topological nature arising from the network structure in the dynamics has not been fully accounted for. Note that conventional speed limits, which read as $\tau \geq \mathcal{L}(\boldsymbol{x}_0, \boldsymbol{x}_\tau)/\bar{v}$, employed nontopological metrics $\mathcal{L}$, such as the Bures angle, trace norm, quantum Fisher information, etc., to quantify the distance between the initial and final states [37]. These metrics are always upper bounded by a constant that does not scale with the size of the system, whereas the dynamics strongly depends on the system size. Velocity $\bar{v}$ is determined by the entire dynamics of the system [51], and hence it is generally of the order of system size. Consequently, conventional speed limits become trivial (i.e., $\tau \geq \mathcal{L}(\boldsymbol{x}_0, \boldsymbol{x}_\tau)/\bar{v} \to 0$) as the system increases in terms of size [52]. This indicates that in order to derive meaningful bounds, metrics that capture the topological nature and are scalable with system size should be considered.

In this Letter, we derive a speed limit for arbitrary states $\boldsymbol{x}_t$ using a topological metric defined through the network structure in the dynamics. The time evolution of such states is described by a graph in which each vertex exchanges flows with each other and may be pumped by an external flow. Examples include the probability distribution of discrete systems, mass concentrations in chemical reaction networks, and vectors of observables in quantum systems (see Fig. 1 again for illustration). We employ a generalized version of the discrete Wasserstein distance to quantify the

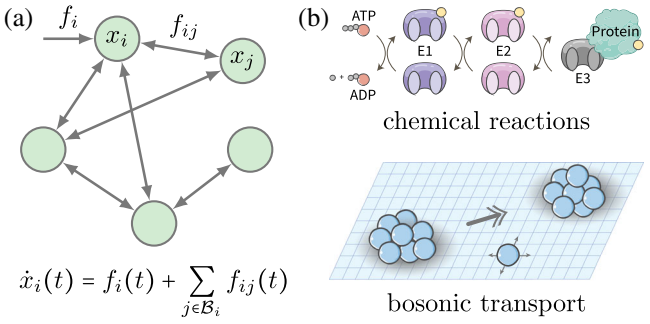

FIG. 1. (a) Generic time evolution of a physical state $\boldsymbol{x}_t = [x_1(t), \ldots, x_N(t)]^\top$ on a graph. $x_i(t)$ is evolved because of the flows $\{f_{ij}(t)\}$ exchanged between neighboring vertices and an external flow $f_i(t)$. (b) Examples include reactant concentrations in deterministic chemical reactions and boson numbers in interacting bosonic systems.

distance between the states. This distance, widely used in optimal transport theory [53], encodes topological information and can grow proportional to the size of the system. We prove that the minimum operational time required to change the physical state is lower bounded by the Wasserstein distance divided by the average velocity [cf. Eqs. (5) and (6)]. The obtained speed limit is tight and can be saturated, even when the system size increases. Moreover, it is applicable to a broad range of dynamics ranging from deterministic and stochastic classical systems to isolated and open quantum systems. For example, we apply the theory to chemical reaction networks using the Wasserstein distance applicable to any reversible chemical reaction and provide a reaction speed formula that can discriminate between different chemical reactions [54]. Another important application is the interacting bosonic transport for arbitrary initial (mixed) states with and without a thermal environment, which is relevant to the Lieb–Robinson velocity [56]. Through the examples, we demonstrate that considering topological metrics does not only provide quantitatively tight bounds but also qualitatively reveals the physical mechanism of state transformations, which cannot be obtained with speed limits reported thus far.

General setup.—We consider a time-dependent vector state $\boldsymbol{x}_t \coloneqq [x_1(t), \ldots, x_N(t)]^\top$ and an undirected graph $G(\mathcal{V}, \mathcal{E})$ with the vertex set $\mathcal{V} = \{1, \ldots, N\}$ and edge set $\mathcal{E}$. Each element $x_i(t)$ corresponds to a vertex $i \in \mathcal{V}$. For example, $\boldsymbol{x}_t$ can be a vector of the probability distribution of a discrete system, reactant concentrations of chemical reaction networks, or physical observables in classical and quantum systems (examples are provided later). For each vertex i, let $\mathcal{B}_i \coloneqq \{j | \langle i, j\rangle \in \mathcal{E}\}$ denote the set of neighboring vertices of i. We assume that the time evolution of $\boldsymbol{x}_t$ is given by the following deterministic equation [see Fig. 1(a)]:

$$\dot{x}_i(t) = f_i(t) + \sum_{j \in \mathcal{B}_i} f_{ij}(t), \tag{1}$$

where $f_{ij}(t) = -f_{ji}(t)$ denotes the flow exchange between vertices i and j for $i \neq j$ and $f_i(t)$ is an arbitrary external flow. In the absence of external flows [i.e., $f_i(t) = 0$ for all i], $\sum_{i=1}^N x_i(t)$ is invariant. Examples of Eq. (1) include the master equation of Markov jump processes, rate equation of chemical reaction networks, and time evolution of the observables in quantum systems. We define a time-dependent velocity [57], which is the sum of the absolute values of the external and exchanged flows, given by

$$\upsilon_{t,\lambda} \coloneqq \lambda \sum_i |f_i(t)| + \sum_{\langle i,j\rangle \in \mathcal{E}} |f_{ij}(t)|, \tag{2}$$

where $\lambda \geq 0$ is a weighting factor, and the second summation is over all unordered pairs $\langle i, j\rangle \in \mathcal{E}$. For simplicity, we denote $\upsilon_{t,0}$ by υ_t. We also define the Manhattan norm for an arbitrary vector $\boldsymbol{x}$ as $\|\boldsymbol{x}\|_1 \coloneqq \sum_i |x_i|$ and the time average of an arbitrary time-dependent quantity w_t as $\langle w_t \rangle_\tau \coloneqq \tau^{-1} \int_0^\tau w_t dt$.

Wasserstein distance.—Here we introduce the discrete L^1-Wasserstein distance between two states $\boldsymbol{x}$ and $\boldsymbol{y}$ on the graph $G(\mathcal{V}, \mathcal{E})$. First, we consider the case in which $\boldsymbol{x}$ and $\boldsymbol{y}$ are balanced (that is, $\sum_i x_i = \sum_i y_i$), and then we generalize the distance to the unbalanced case (that is, $\sum_i x_i \neq \sum_i y_i$). Let d_{ij} denote the shortest path distance between the vertices i and j in the graph. In other words, d_{ij} is the minimum length of paths connecting i and j. Graph G is assumed to be connected [59]; therefore, d_{ij} is always finite. Suppose that we have a transport plan that redistributes $\boldsymbol{x}$ to $\boldsymbol{y}$ by sending an amount of π_{ij} from x_j to y_i with a cost of d_{ij} per unit weight for all ordered pairs $\langle i, j\rangle$. The Wasserstein distance is then defined as the minimum transport cost for all feasible plans, given by

$$\mathcal{W}_1(\boldsymbol{x}, \boldsymbol{y}) \coloneqq \min_{\pi \in \Pi(\boldsymbol{x}, \boldsymbol{y})} \sum_{i,j} d_{ij} \pi_{ij}. \tag{3}$$

Here, $\Pi(\boldsymbol{x}, \boldsymbol{y})$ denotes the set of all transport plans $\pi = [\pi_{ij}] \in \mathbb{R}_{\geq 0}^{N \times N}$ that satisfy $\sum_j \pi_{ij} = y_i$ and $\sum_j \pi_{ji} = x_i$. Previous studies have shown that the Wasserstein distance plays a crucial role in statistics and machine learning [60], computer vision [61], linguistics [62], molecular biology [63], and stochastic thermodynamics [33,64–66].

Next, we describe the generalized Wasserstein distance for the unbalanced case. Transport between two unbalanced states can be enabled by allowing *add* and *remove* operations in addition to transportation between vertices. More precisely, an infinitesimal mass $\delta\boldsymbol{x}$ of $\boldsymbol{x}$ can either be removed at cost $\lambda \|\delta\boldsymbol{x}\|_1$ or moved from $\boldsymbol{x}$ to $\boldsymbol{y}$ at cost $\mathcal{W}_1(\delta\boldsymbol{x}, \delta\boldsymbol{y})$. Mathematically, the generalized Wasserstein distance between unbalanced states can be defined as [67]

$$\mathcal{W}_{1,\lambda}(\boldsymbol{x}, \boldsymbol{y}) \coloneqq \min\{\lambda(\|\boldsymbol{x} - \tilde{\boldsymbol{x}}\|_1 + \|\boldsymbol{y} - \tilde{\boldsymbol{y}}\|_1) + \mathcal{W}_1(\tilde{\boldsymbol{x}}, \tilde{\boldsymbol{y}})\}, \tag{4}$$

where the minimum is over all the states $\tilde{\boldsymbol{x}}$ and $\tilde{\boldsymbol{y}}$ such that $\|\tilde{\boldsymbol{x}}\|_1 = \|\tilde{\boldsymbol{y}}\|_1$. By definition [Eq. (4)], distance $\mathcal{W}_{1,\lambda}$ always satisfies the triangle inequality [67]. If $\boldsymbol{x}$ and $\boldsymbol{y}$ are balanced states, then $\mathcal{W}_{1,\lambda}$ is reduced to $\mathcal{W}_1$ within the $\lambda \to +\infty$ limit. We also note that $\mathcal{W}_{1,\lambda}$ can be calculated numerically using the linear programming method [68].

Main results.—We now utilize the generalized Wasserstein distance [Eq. (4)] to derive a topological speed limit for any state $\boldsymbol{x}_t$ obeying the general dynamics [Eq. (1)]. Specifically, we prove that the minimum time required to transform $\boldsymbol{x}_0$ into $\boldsymbol{x}_\tau$ is lower bounded by the Wasserstein distance divided by the average velocity

$$\tau \geq \frac{\mathcal{W}_{1,\lambda}(\boldsymbol{x}_0, \boldsymbol{x}_\tau)}{\langle \upsilon_{t,\lambda} \rangle_\tau}, \quad \forall\, \lambda \geq 0. \tag{5}$$

In the case that the external flows are absent [i.e., $f_i(t) = 0$], inequality (5) can be reduced to a simple bound by taking the $\lambda \to +\infty$ limit, which reads as

$$\tau \geq \frac{\mathcal{W}_1(\boldsymbol{x}_0, \boldsymbol{x}_\tau)}{\langle v_t \rangle_\tau}. \tag{6}$$

The inequalities [Eqs. (5) and (6)] are our main results; the proof is postponed to the end of the Letter.

These results have several physically critical properties. (i) First, these bounds can be derived as long as the time evolution of $\boldsymbol{x}_t$ is described by Eq. (1), which is a general setting for both the classical and quantum cases. Notably, the bounds can be saturated if the time evolution [Eq. (1)] realizes an optimal transport plan. (ii) Second, our bounds utilize topological information about the system dynamics to provide a stringent constraint on the speed of changing states. Topological information is encoded into the Wasserstein distance, and this distance term can be as large as the order of the system's size. (iii) Third, by further upper bounding the time-averaged velocity $\langle v_{t,\lambda} \rangle_\tau$ by relevant quantities, such as the thermodynamic and kinetic costs, we can derive more interpretable bounds, which clarify the physical mechanism of the speed of state transformations. (iv) Finally, the speed limit for an arbitrary scalar observable defined in terms of state $\boldsymbol{x}_t$ can also be obtained as a consequence of Eq. (5) [68].

In the following, we illustrate the above remarks, especially (i)–(iii), through two applications to classical and quantum systems (see the Supplemental Material [68] for further applications in isolated and Markovian open quantum systems, measurement-induced quantum walk [71], and quantum communication [72,73]).

Application 1: Chemical reaction networks.—We consider a chemical reaction system composed of several chemical species X_i ($i \in \mathcal{S}$) that interact through reversible elementary reaction channels $\rho \in \mathcal{R}$. Here, $\mathcal{S}$ and $\mathcal{R}$ denote the set of indices of the species and reaction channels, respectively. Each reaction channel is represented as

$$\sum_i \nu_i^{+\rho} X_i \underset{\kappa^{-\rho}}{\overset{\kappa^{+\rho}}{\rightleftharpoons}} \sum_i \nu_i^{-\rho} X_i, \tag{7}$$

where $+\rho$ and $-\rho$ correspond to the forward and backward reactions, respectively, $\{\kappa^{\pm\rho}\}$ are the macroscopic reaction rates, and $\{\nu_i^{\pm\rho}\}$ are the stoichiometric coefficients. Let $\boldsymbol{x}_t$ denote the vector of the mass concentrations of species. The molar concentration $\boldsymbol{c}_t$ can be related as $c_i(t) = x_i(t)/m_i$, where m_i denotes the molar mass of species X_i. The time evolution of $\boldsymbol{x}_t$ can be described by the deterministic rate equation

$$\dot{x}_i(t) = \sum_\rho m_i(\nu_i^{+\rho} - \nu_i^{-\rho}) J_t^\rho, \tag{8}$$

where $J_t^\rho := J_t^{-\rho} - J_t^{+\rho}$ is the net reaction current and $J_t^{\pm\rho} := \kappa^{\pm\rho} \prod_i c_i(t)^{\nu_i^{\pm\rho}}$ are the reaction fluxes.

Next, we derive the speed limits for the system in terms of the Wasserstein distance defined on graph G. For simplicity, here we consider closed reaction networks, in which the total mass concentration is conserved [74]. The generalization for open reaction networks, wherein the total mass conservation may be violated, is presented in the Supplemental Material [68]. The total mass conservation law implies $\sum_i m_i(\nu_i^{+\rho} - \nu_i^{-\rho}) = 0$ for any ρ. Because of these conditions, there always exist matrices $\boldsymbol{Z}^\rho = [z_{ij}^\rho]$ such that the rate equation (8) can be expressed in the form of Eq. (1) with $f_{ij}(t) = \sum_\rho z_{ij}^\rho J_t^\rho$ and $f_i(t) = 0$ [68]. The graph G can be obtained by adding an undirected edge $\langle i, j \rangle$ to $\mathcal{E}$ for any $z_{ij}^\rho \neq 0$. After some simple manipulations [68], we can prove that

$$v_t \leq \sum_\rho \nu^\rho |J_t^\rho|, \tag{9}$$

where $\nu^\rho := (1/2) \sum_i m_i |\nu_i^{+\rho} - \nu_i^{-\rho}|$. Combining Eqs. (6) and (9) yields the following speed limit:

$$\tau \geq \frac{\mathcal{W}_1(\boldsymbol{x}_0, \boldsymbol{x}_\tau)}{\langle \sum_\rho \nu^\rho |J_t^\rho| \rangle_\tau} =: \tau_1. \tag{10}$$

Equation (10) implies that the operational time is lower bounded by the Wasserstein distance and the net reaction currents.

A thermodynamic speed limit can also be obtained using Eq. (10). The entropy production rate of a chemical reaction system can be defined as [76]

$$\sigma_t := \sum_\rho J_t^\rho \ln \frac{J_t^{-\rho}}{J_t^{+\rho}}, \tag{11}$$

where the gas constant is set to unity. We define the following kinetic quantity:

$$\ell_t := \sum_\rho (\nu^\rho)^2 \frac{J_t^{-\rho} - J_t^{+\rho}}{\ln(J_t^{-\rho}/J_t^{+\rho})}, \tag{12}$$

which is the sum of the microscopic Onsager coefficients [33,55]. Applying the Cauchy–Schwarz inequality, we prove that $\langle \sum_\rho \nu^\rho |J_t^\rho| \rangle_\tau \leq \langle \sqrt{\sigma_t \ell_t} \rangle_\tau \leq \sqrt{\langle \sigma_t \rangle_\tau \langle \ell_t \rangle_\tau}$. Consequently, we obtain the following thermodynamic speed limit:

$$\tau \geq \frac{\mathcal{W}_1(\boldsymbol{x}_0, \boldsymbol{x}_\tau)}{\sqrt{\langle \sigma_t \rangle_\tau \langle \ell_t \rangle_\tau}} =: \tau_2. \tag{13}$$

Inequality (13) implies that the minimum time required to transform $\boldsymbol{x}_0$ into $\boldsymbol{x}_\tau$ is determined by the product of the thermodynamic and kinetic costs.

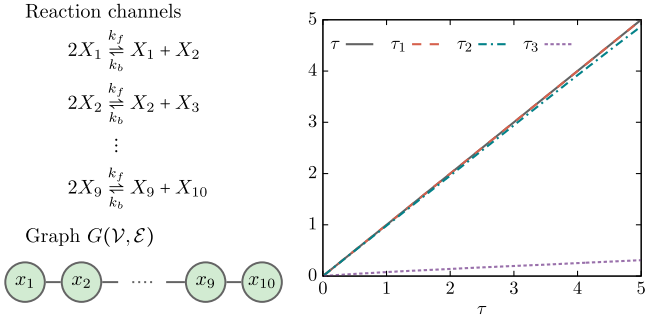

FIG. 2. Numerical demonstration of the speed limits in the cascade reaction network with $N = 10$. The operational time τ, topological bounds τ_1 and τ_2, and nontopological bound τ_3 are depicted by solid, dashed and dash-dotted, and dotted lines, respectively. The parameters are set to $k_f = 2$ and $k_b = 1$. The initial mass concentration is $\boldsymbol{x}_0 = [1, 0.9, \ldots, 0.1]^\top$.

We numerically demonstrate the derived bounds in a cascade reaction network with $|\mathcal{S}| = 10$ species and $|\mathcal{R}| = 9$ reaction channels (see Fig. 2). We also compare the results with a nontopological bound reported in Ref. [77], which reads as $\tau \geq \tau_3 := \mathcal{T}(\boldsymbol{c}_0, \boldsymbol{c}_\tau)/\sqrt{\langle \sigma_t \rangle_\tau \langle d_t \rangle_\tau}$. Here, $\mathcal{T}$ denotes the total variation distance, and $d_t := (|\mathcal{S}|/8)\sum_{\rho,i}(\nu_i^{+\rho} - \nu_i^{-\rho})^2(J_t^{+\rho} + J_t^{-\rho})$ corresponds to the diffusion coefficient. We calculate and plot the lower bounds $\tau_i (1 \leq i \leq 3)$ in Fig. 2. As shown, the topological speed limits $\tau \geq \tau_1 \geq \tau_2$ are tight; especially, the bound $\tau \geq \tau_1$ is always saturated. On the contrary, the nontopological bound $\tau \geq \tau_3$ is loose and does not provide a meaningful bound for the speed of the system.

Application 2: Interacting bosonic systems.—Next, we describe an application for quantum many-body bosonic systems. We consider a model of bosons that hop on an arbitrary finite-dimensional lattice and interact with each other. Let Λ denote the set of all the sites in the lattice. The Hamiltonian can be expressed in the following generic form:

$$H_t := -\gamma \sum_{\langle i,j \rangle} (b_i^\dagger b_j + b_j^\dagger b_i) + \sum_{Z \subseteq \Lambda} h_Z. \tag{14}$$

Here, the first summation is over neighboring lattice sites (which can be arbitrarily distant), $\gamma > 0$ describes the boson mobility, b_i and $b_i^\dagger$ are the bosonic annihilation and creation operators for site i, respectively, $\hat{n}_i := b_i^\dagger b_i$ is the number operator, and h_Z is an arbitrary function of $\{\hat{n}_i\}_{i \in Z}$. Examples include the Bose–Hubbard model, given by $\sum_{Z \subseteq \Lambda} h_Z = (U/2)\sum_i \hat{n}_i(\hat{n}_i - 1) - \mu \sum_i \hat{n}_i$, where U and μ are real constants. Note that the graph $G(\mathcal{V},\mathcal{E})$ of the bosonic system is identical to the lattice topology (i.e., $\mathcal{V}$ is the set of sites, and $\mathcal{E}$ is the set of edges that connect the two neighboring sites). The maximum vertex degree of the graph is denoted by d_G.

We assume that the bosonic system is weakly coupled to a Markovian thermal reservoir and can exchange particles with the reservoir, where the time evolution of the reduced density matrix is described by the Lindblad equation [78]:

$$\dot{\varrho}_t = -i[H_t, \varrho_t] + \sum_{i \in \Lambda} (\mathcal{D}[L_{i,+}] + \mathcal{D}[L_{i,-}])\varrho_t, \tag{15}$$

where $\mathcal{D}[L]\varrho := L\varrho L^\dagger - (1/2)\{L^\dagger L, \varrho\}$ is the dissipator, and $L_{i,+} = \sqrt{\gamma_{i,+}} b_i^\dagger$ and $L_{i,-} = \sqrt{\gamma_{i,-}} b_i$ are the jump operators that characterize the absorption and emission of bosons at site i, respectively. Hereafter, we set $\hbar = 1$ for simplicity.

We consider the vector of boson numbers occupied at each site, $x_i(t) = \mathrm{tr}\{\hat{n}_i \varrho_t\}$, and define the instantaneous total number of bosons as $\mathcal{N}_t := \sum_{i \in \Lambda} x_i(t)$. Using the relation $[b_i, \hat{n}_i] = b_i$, we can show that the time evolution of $x_i(t)$ can be expressed in the form of Eq. (1) with $f_i(t) = \mathrm{tr}\{L_{i,+}\varrho_t L_{i,+}^\dagger\} - \mathrm{tr}\{L_{i,-}\varrho_t L_{i,-}^\dagger\}$ and $f_{ij}(t) = 2\gamma \mathrm{Im}[\mathrm{tr}\{b_j^\dagger b_i \varrho_t\}]$. By inserting these terms into $\upsilon_{t,\lambda}$, we can immediately obtain the speed limit [Eq. (5)] for bosonic transport.

Next, we derive a more physically interpretable speed limit by upper bounding the velocity $\upsilon_{t,\lambda}$. To this end, we introduce two relevant physical quantities. The first is the irreversible entropy production rate [79], which is the sum of the entropic changes in the system and environment, defined as $\sigma_t := \sigma_t^{\mathrm{sys}} + \sigma_t^{\mathrm{env}}$. Here, $\sigma_t^{\mathrm{sys}} := -\mathrm{tr}\{\dot{\varrho}_t \ln \varrho_t\}$ is the rate of von Neumann entropy of the bosonic system, and σ_t^{env} quantifies the heat dissipated to the environment as follows:

$$\sigma_t^{\mathrm{env}} := \sum_i (\mathrm{tr}\{L_{i,+}\varrho_t L_{i,+}^\dagger\} - \mathrm{tr}\{L_{i,-}\varrho_t L_{i,-}^\dagger\}) \ln \frac{\gamma_{i,+}}{\gamma_{i,-}}, \tag{16}$$

where we have assumed the local detailed balance condition [that is, $\ln(\gamma_{i,+}/\gamma_{i,-})$ is related to the heat dissipation of the boson exchange at site i]. The second is quantum dynamical activity [80,81], which quantifies the boson exchange frequency between the system and reservoir, given by

$$a_t := \sum_i (\mathrm{tr}\{L_{i,+}\varrho_t L_{i,+}^\dagger\} + \mathrm{tr}\{L_{i,-}\varrho_t L_{i,-}^\dagger\}). \tag{17}$$

Using these quantities, we can prove that the velocity $\upsilon_{t,\lambda}$ is upper bounded as [68]

$$\upsilon_{t,\lambda} \leq \gamma d_G \mathcal{N}_t + \lambda \frac{\sigma_t}{2} \Phi\left(\frac{\sigma_t}{2a_t}\right)^{-1}, \tag{18}$$

where $\Phi(x)$ is the inverse function of $x\tanh(x)$. By combining Eqs. (5) and (18), we obtain the following speed limit:

$$\tau \geq \frac{\mathcal{W}_{1,\lambda}(\boldsymbol{x}_0, \boldsymbol{x}_\tau)}{\langle \gamma d_G \mathcal{N}_t + \lambda \sigma_t \Phi(\sigma_t/2a_t)^{-1}/2 \rangle_\tau}. \tag{19}$$

Equation (19) implies that the speed of bosonic transport is lower bounded by the lattice topology, boson mobility, and dissipation. The bound also indicates that dissipative controls can help accelerate the bosonic transport. The inequality [Eq. (19)] is valid for arbitrary initial states of the bosonic system.

It is worthwhile discussing the vanishing coupling limit (i.e., the case where the system becomes isolated). In this case, $\sigma_t = a_t = 0$ and $\mathcal{N}_t = \mathcal{N}$ for all times. Defining the boson concentration $\bar{x}_i(t) \coloneqq \mathcal{N}^{-1} x_i(t)$, we obtain $\sum_i \bar{x}_i(t) = 1$. By taking the $\lambda \to +\infty$ limit, Eq. (19) is reduced to a simple speed limit for an isolated bosonic system:

$$\tau \geq \frac{\mathcal{W}_1(\bar{\boldsymbol{x}}_0, \bar{\boldsymbol{x}}_\tau)}{\gamma d_G}. \tag{20}$$

Bound (20) has a remarkable implication for bosonic transport. Assume that all bosons are initially concentrated in a region R_1, and we want to transport all of them to a distinct region R_2 within a finite time τ. In this case, $\mathcal{W}_1(\bar{\boldsymbol{x}}_0, \bar{\boldsymbol{x}}_\tau) \geq \mathrm{dist}(R_1, R_2)$, where $\mathrm{dist}(R_1, R_2)$ denotes the length of the shortest path connecting the regions R_1 and R_2. Therefore, Eq. (20) implies that transporting bosons always takes at least a time proportional to the distance between the two regions: $\tau \geq \mathrm{dist}(R_1, R_2)/(\gamma d_G)$, which cannot be obtained with conventional speed limits. This statement holds for *arbitrary* initial states, including the pure states considered in Ref. [82]. While the Lieb–Robinson bounds [83–87] imply a linear light cone for the operator spreading, Eq. (20) provides a useful bound for the operational time required for bosonic transport.

Proof of Eq. (5).—We consider the time discretization of Eq. (1) with time interval $\delta t = \tau/K$. For each $k \in [0, K-1]$ and $t = k\delta t$, we have

$$x_i(t+\delta t) = x_i(t) + \delta t \left[f_i(t) + \sum_{j \in \mathcal{B}_i} f_{ij}(t) \right]. \tag{21}$$

Equation (21) indicates that we can transform $\boldsymbol{x}_t$ into $\boldsymbol{x}_{t+\delta t}$ by adding $f_i(t)\delta t$ to $x_i(t)$ with cost $\lambda |f_i(t)| \delta t$ and exchanging $f_{ij}(t)\delta t$ between neighboring vertices i and j with cost $|f_{ij}(t)|\delta t$. This instance of transport plan takes the total cost of

$$\left(\lambda \sum_i |f_i(t)| + \sum_{\langle i,j \rangle \in \mathcal{E}} |f_{ij}(t)| \right) \delta t = \upsilon_{t,\lambda} \delta t, \tag{22}$$

which should be larger than or equal to $\mathcal{W}_{1,\lambda}(\boldsymbol{x}_t, \boldsymbol{x}_{t+\delta t})$. Therefore, taking the sum of Eq. (22) from $k = 0$ to $k = K-1$ and applying the triangle inequality for $\mathcal{W}_{1,\lambda}$ yield

$$\sum_{k=0}^{K-1} \upsilon_{t,\lambda} \delta t \geq \mathcal{W}_{1,\lambda}(\boldsymbol{x}_0, \boldsymbol{x}_\tau). \tag{23}$$

By taking the $\delta t \to 0$ limit in Eq. (23), we obtain $\tau \langle \upsilon_{t,\lambda} \rangle_\tau \geq \mathcal{W}_{1,\lambda}(\boldsymbol{x}_0, \boldsymbol{x}_\tau)$, from which Eq. (5) is immediately derived.

Conclusion.—In this Letter, we derived the topological speed limit for vector states that accounts for the network structure in the underlying dynamics [88]. The speed limit provides a tight bound for the operational time and insight into the system speed from a topological perspective. We showed that the bound is applicable to various dynamics as long as the time evolution of the physical state can be described in terms of a graph. Because our speed limit is derived in a general setting, we expect that it can be applied to obtain fundamental bounds for several other dynamics.

We thank Tomotaka Kuwahara, Andreas Dechant, and Koudai Sugimoto for fruitful discussions; Marius Lemm and Ryusuke Hamazaki for helpful communications; and Mai Dan Nguyen for help in preparing the figures. We also appreciate anonymous referees for valuable comments. This work was supported by Grants-in-Aid for Scientific Research (No. JP19H05603 and No. JP19H05791).

*tanvu@rk.phys.keio.ac.jp
†saitoh@rk.phys.keio.ac.jp

[1] L. Mandelstam and I. Tamm, The uncertainty relation between energy and time in non-relativistic quantum mechanics, J. Phys. USSR **9**, 249 (1945).
[2] A. Uhlmann, An energy dispersion estimate, Phys. Lett. A **161**, 329 (1992).
[3] N. Margolus and L. B. Levitin, The maximum speed of dynamical evolution, Physica (Amsterdam) **120D**, 188 (1998).
[4] A. del Campo, I. L. Egusquiza, M. B. Plenio, and S. F. Huelga, Quantum Speed Limits in Open System Dynamics, Phys. Rev. Lett. **110**, 050403 (2013).
[5] S. Deffner and E. Lutz, Quantum Speed Limit for Non-Markovian Dynamics, Phys. Rev. Lett. **111**, 010402 (2013).
[6] M. M. Taddei, B. M. Escher, L. Davidovich, and R. L. de Matos Filho, Quantum Speed Limit for Physical Processes, Phys. Rev. Lett. **110**, 050402 (2013).
[7] D. P. Pires, M. Cianciaruso, L. C. Céleri, G. Adesso, and D. O. Soares-Pinto, Generalized Geometric Quantum Speed Limits, Phys. Rev. X **6**, 021031 (2016).
[8] D. Mondal, C. Datta, and S. Sazim, Quantum coherence sets the quantum speed limit for mixed states, Phys. Lett. A **380**, 689 (2016).
[9] S. Deffner, Geometric quantum speed limits: A case for Wigner phase space, New J. Phys. **19**, 103018 (2017).
[10] B. Shanahan, A. Chenu, N. Margolus, and A. del Campo, Quantum Speed Limits across the Quantum-to-Classical Transition, Phys. Rev. Lett. **120**, 070401 (2018).
[11] M. Okuyama and M. Ohzeki, Quantum Speed Limit is not Quantum, Phys. Rev. Lett. **120**, 070402 (2018).
[12] S. Ito, Stochastic Thermodynamic Interpretation of Information Geometry, Phys. Rev. Lett. **121**, 030605 (2018).

[13] N. Shiraishi, K. Funo, and K. Saito, Speed Limit for Classical Stochastic Processes, Phys. Rev. Lett. **121**, 070601 (2018).
[14] F. Campaioli, F. A. Pollock, F. C. Binder, and K. Modi, Tightening Quantum Speed Limits for almost all States, Phys. Rev. Lett. **120**, 060409 (2018).
[15] K. Funo, N. Shiraishi, and K. Saito, Speed limit for open quantum systems, New J. Phys. **21**, 013006 (2019).
[16] L. P. García-Pintos and A. del Campo, Quantum speed limits under continuous quantum measurements, New J. Phys. **21**, 033012 (2019).
[17] T. D. Kieu, A class of time-energy uncertainty relations for time-dependent Hamiltonians, Proc. R. Soc. A **475**, 20190148 (2019).
[18] X. Hu, S. Sun, and Y. Zheng, Quantum speed limit via the trajectory ensemble, Phys. Rev. A **101**, 042107 (2020).
[19] S. Ito and A. Dechant, Stochastic Time Evolution, Information Geometry, and the Cramér-Rao Bound, Phys. Rev. X **10**, 021056 (2020).
[20] S. B. Nicholson, L. P. García-Pintos, A. del Campo, and J. R. Green, Time-information uncertainty relations in thermodynamics, Nat. Phys. **16**, 1211 (2020).
[21] V. T. Vo, T. Van Vu, and Y. Hasegawa, Unified approach to classical speed limit and thermodynamic uncertainty relation, Phys. Rev. E **102**, 062132 (2020).
[22] T. Fogarty, S. Deffner, T. Busch, and S. Campbell, Orthogonality Catastrophe as a Consequence of the Quantum Speed Limit, Phys. Rev. Lett. **124**, 110601 (2020).
[23] N. Il'in and O. Lychkovskiy, Quantum speed limit for thermal states, Phys. Rev. A **103**, 062204 (2021).
[24] S. Sun, Y. Peng, X. Hu, and Y. Zheng, Quantum Speed Limit Quantified by the Changing Rate of Phase, Phys. Rev. Lett. **127**, 100404 (2021).
[25] T. Van Vu and Y. Hasegawa, Geometrical Bounds of the Irreversibility in Markovian Systems, Phys. Rev. Lett. **126**, 010601 (2021).
[26] E. O'Connor, G. Guarnieri, and S. Campbell, Action quantum speed limits, Phys. Rev. A **103**, 022210 (2021).
[27] N. Shiraishi and K. Saito, Speed limit for open systems coupled to general environments, Phys. Rev. Res. **3**, 023074 (2021).
[28] K. Bolonek-Lasoń, J. Gonera, and P. Kosiński, Classical and quantum speed limits, Quantum **5**, 482 (2021).
[29] A. del Campo, Probing Quantum Speed Limits with Ultracold Gases, Phys. Rev. Lett. **126**, 180603 (2021).
[30] J.-C. Delvenne and G. Falasco, Tight classical speed limits, arXiv:2110.13050.
[31] R. Hamazaki, Speed limits for macroscopic transitions, PRX Quantum **3**, 020319 (2022).
[32] Y. Hasegawa, Thermodynamic bounds via bulk-boundary correspondence: Speed limit, thermodynamic uncertainty relation, and Heisenberg principle, arXiv:2203.12421.
[33] T. Van Vu and K. Saito, Thermodynamic unification of optimal transport: Thermodynamic uncertainty relation, minimum dissipation, and thermodynamic speed limits, arXiv:2206.02684.
[34] S. Nakajima and Y. Utsumi, Speed limits of the trace distance in the interaction picture for open quantum system, New. J. Phys. **24**, 095004 (2022).
[35] D. S. P. Salazar, Lower bound for entropy production rate in stochastic systems far from equilibrium, Phys. Rev. E **106**, L032101 (2022).
[36] A. Kolchinsky, A. Dechant, K. Yoshimura, and S. Ito, Information geometry of excess and housekeeping entropy production, arXiv:2206.14599.
[37] S. Deffner and S. Campbell, Quantum speed limits: From Heisenberg's uncertainty principle to optimal quantum control, J. Phys. A **50**, 453001 (2017).
[38] T. Caneva, M. Murphy, T. Calarco, R. Fazio, S. Montangero, V. Giovannetti, and G. E. Santoro, Optimal Control at the Quantum Speed Limit, Phys. Rev. Lett. **103**, 240501 (2009).
[39] S. Deffner, Optimal control of a qubit in an optical cavity, J. Phys. B **47**, 145502 (2014).
[40] S. Campbell and S. Deffner, Trade-Off between Speed and Cost in Shortcuts to Adiabaticity, Phys. Rev. Lett. **118**, 100601 (2017).
[41] K. Funo, J.-N. Zhang, C. Chatou, K. Kim, M. Ueda, and A. del Campo, Universal Work Fluctuations During Shortcuts to Adiabaticity by Counterdiabatic Driving, Phys. Rev. Lett. **118**, 100602 (2017).
[42] V. Giovannetti, S. Lloyd, and L. Maccone, Quantum Metrology, Phys. Rev. Lett. **96**, 010401 (2006).
[43] M. Beau and A. del Campo, Nonlinear Quantum Metrology of Many-Body Open Systems, Phys. Rev. Lett. **119**, 010403 (2017).
[44] S. Lloyd, Ultimate physical limits to computation, Nature (London) **406**, 1047 (2000).
[45] K. Proesmans, J. Ehrich, and J. Bechhoefer, Finite-Time Landauer Principle, Phys. Rev. Lett. **125**, 100602 (2020).
[46] S. Deffner, Energetic cost of Hamiltonian quantum gates, Europhys. Lett. **134**, 40002 (2021).
[47] Y.-Z. Zhen, D. Egloff, K. Modi, and O. Dahlsten, Universal Bound on Energy Cost of Bit Reset in Finite Time, Phys. Rev. Lett. **127**, 190602 (2021).
[48] T. Van Vu and K. Saito, Finite-Time Quantum Landauer Principle and Quantum Coherence, Phys. Rev. Lett. **128**, 010602 (2022).
[49] J. S. Lee, S. Lee, H. Kwon, and H. Park, Speed Limit for a Highly Irreversible Process and Tight Finite-Time Landauer's Bound, Phys. Rev. Lett. **129**, 120603 (2022).
[50] J. Eisert, M. van den Worm, S. R. Manmana, and M. Kastner, Breakdown of Quasilocality in Long-Range Quantum Lattice Models, Phys. Rev. Lett. **111**, 260401 (2013).
[51] F. Campaioli, F. A. Pollock, and K. Modi, Tight, robust, and feasible quantum speed limits for open dynamics, Quantum **3**, 168 (2019).
[52] M. Bukov, D. Sels, and A. Polkovnikov, Geometric Speed Limit of Accessible Many-Body State Preparation, Phys. Rev. X **9**, 011034 (2019).
[53] C. Villani, *Optimal Transport: Old and New* (Springer, Berlin, Heidelberg, 2008).
[54] We note the related work [55] which discusses the application of Wasserstein distance to chemical reactions. However, this study uses the system-dependent L^2-Wasserstein distance [25], which is defined for a given fixed chemical reaction system. Therefore, the reaction speeds cannot be compared between different chemical reactions.

[55] K. Yoshimura, A. Kolchinsky, A. Dechant, and S. Ito, Geometrical approach to excess/housekeeping entropy production in discrete systems, arXiv:2205.15227.
[56] E. H. Lieb and D. W. Robinson, The finite group velocity of quantum spin systems, Commun. Math. Phys. **28**, 251 (1972).
[57] Note that this velocity, which contains the absolute value of currents, is qualitatively and quantitatively different from dynamical activity in the literature, which involves the absolute value of unidirectional fluxes [58].
[58] C. Maes, Frenesy: Time-symmetric dynamical activity in nonequilibria, Phys. Rep. **850**, 1 (2020).
[59] A graph is said to be connected if there always exists a path from any vertex to any other vertex in the graph. In the case that the graph is not connected, we can define the Wasserstein distance as the sum of the distances defined for each connected component.
[60] S. Kolouri, S. R. Park, M. Thorpe, D. Slepcev, and G. K. Rohde, Optimal mass transport: Signal processing and machine-learning applications, IEEE Signal Process. Mag. **34**, 43 (2017).
[61] S. Haker, L. Zhu, A. Tannenbaum, and S. Angenent, Optimal mass transport for registration and warping, Int. J. Comput. Vis. **60**, 225 (2004).
[62] G. Huang, C. Guo, M. J. Kusner, Y. Sun, F. Sha, and K. Q. Weinberger, Supervised word mover's distance, in *Advances in Neural Information Processing Systems* (Curran Associates, Inc., Spain, 2016), Vol. 29.
[63] G. Schiebinger, J. Shu, M. Tabaka, B. Cleary, V. Subramanian, A. Solomon, J. Gould, S. Liu, S. Lin, P. Berube *et al.*, Optimal-transport analysis of single-cell gene expression identifies developmental trajectories in reprogramming, Cell **176**, 928 (2019).
[64] E. Aurell, C. Mejía-Monasterio, and P. Muratore-Ginanneschi, Optimal Protocols and Optimal Transport in Stochastic Thermodynamics, Phys. Rev. Lett. **106**, 250601 (2011).
[65] M. Nakazato and S. Ito, Geometrical aspects of entropy production in stochastic thermodynamics based on Wasserstein distance, Phys. Rev. Res. **3**, 043093 (2021).
[66] A. Dechant, Minimum entropy production, detailed balance and Wasserstein distance for continuous-time Markov processes, J. Phys. A **55**, 094001 (2022).
[67] B. Piccoli and F. Rossi, Generalized Wasserstein distance and its application to transport equations with source, Arch. Ration. Mech. Anal. **211**, 335 (2014).
[68] See Supplemental Material at http://link.aps.org/supplemental/10.1103/PhysRevLett.130.010402 for details of analytical calculations and further applications, which includes Refs. [69,70].
[69] M. Fishman, S. R. White, and E. M. Stoudenmire, The ITensor Software Library for Tensor Network Calculations, SciPost Phys. Codebases, 4 (2022) 10.21468/SciPostPhysCodeb.4.
[70] M. Yang and S. R. White, Time-dependent variational principle with ancillary Krylov subspace, Phys. Rev. B **102**, 094315 (2020).
[71] A. Didi and E. Barkai, Measurement-induced quantum walks, Phys. Rev. E **105**, 054108 (2022).
[72] S. Bose, Quantum Communication through an Unmodulated Spin Chain, Phys. Rev. Lett. **91**, 207901 (2003).
[73] M. Murphy, S. Montangero, V. Giovannetti, and T. Calarco, Communication at the quantum speed limit along a spin chain, Phys. Rev. A **82**, 022318 (2010).
[74] Note that the mass conservation may not be fulfilled in open reaction networks. For example, in the presence of catalysts [75], the total mass concentration may vary over time.
[75] J. Unterberger and P. Nghe, Stoechiometric and dynamical autocatalysis for diluted chemical reaction networks, J. Math. Biol. **85**, 26 (2022).
[76] R. Rao and M. Esposito, Nonequilibrium Thermodynamics of Chemical Reaction Networks: Wisdom from Stochastic Thermodynamics, Phys. Rev. X **6**, 041064 (2016).
[77] K. Yoshimura and S. Ito, Thermodynamic Uncertainty Relation and Thermodynamic Speed Limit in Deterministic Chemical Reaction Networks, Phys. Rev. Lett. **127**, 160601 (2021).
[78] G. Lindblad, On the generators of quantum dynamical semigroups, Commun. Math. Phys. **48**, 119 (1976).
[79] G. T. Landi and M. Paternostro, Irreversible entropy production: From classical to quantum, Rev. Mod. Phys. **93**, 035008 (2021).
[80] Y. Hasegawa, Quantum Thermodynamic Uncertainty Relation for Continuous Measurement, Phys. Rev. Lett. **125**, 050601 (2020).
[81] T. Van Vu and K. Saito, Thermodynamics of Precision in Markovian Open Quantum Dynamics, Phys. Rev. Lett. **128**, 140602 (2022).
[82] J. Faupin, M. Lemm, and I. M. Sigal, Maximal Speed for Macroscopic Particle Transport in the Bose-Hubbard Model, Phys. Rev. Lett. **128**, 150602 (2022).
[83] T. Kuwahara and K. Saito, Lieb-Robinson Bound and almost-Linear Light Cone in Interacting Boson Systems, Phys. Rev. Lett. **127**, 070403 (2021).
[84] M. C. Tran, A. Y. Guo, C. L. Baldwin, A. Ehrenberg, A. V. Gorshkov, and A. Lucas, Lieb-Robinson Light Cone for Power-Law Interactions, Phys. Rev. Lett. **127**, 160401 (2021).
[85] J. Faupin, M. Lemm, and I. M. Sigal, On Lieb–Robinson bounds for the Bose–Hubbard model, Commun. Math. Phys. **394**, 1011 (2022).
[86] C. Yin and A. Lucas, Finite Speed of Quantum Information in Models of Interacting Bosons at Finite Density, Phys. Rev. X **12**, 021039 (2022).
[87] T. Kuwahara, T. Van Vu, and K. Saito, Optimal light cone and digital quantum simulation of interacting bosons, arXiv:2206.14736.
[88] We notice the recent work [31] that has a similar motivation. Note that we consider the speed limits for vector states, which cover a wide range of state transformations, whereas Ref. [31] studies the speed limit only for a fixed scalar observable.